NUMERICAL AND EXPERIMENTAL INVESTIGATIONS OF PASSIVE FLOW CONTROL DEVICES ON A BACKWARD FACING STEP

N.F.Zulkefli, E.N.Tai, M.A. Mujeebu, M.Z.Abdullah, K.A.Ahmad*
School of Mechanical and Aerospace Engineering, Universiti Sains Malaysia, Engineering Campus, Seri Ampangan, 14300 Nibong Tebal, Seberang Perai Selatan, Pulau Pinang, Malaysia.
*E-mail: aekamarul@eng.usm.my

ABSTRACT

A study of passive sub-boundary layer vortex generators (VG) on a backward step surface is presented. Both numerical and experimental analyses are carried out on an array of skewed vane-typed vortex generators. The RANS code FLUENT 6™ is used in the 3D simulations to predict the flow fields using a hybrid mesh with k-ε turbulence model and standard wall function. The flow measurements are made at different flow velocities by using a particle image velocimetry (PIV) system. The results suggest that the passive vortex generators are able to suppress the separation flow region. The comparison between experimental and computational methods reveals a satisfactory agreement.

Keywords: *CFD, backward-facing step, vortex generator*

INTRODUCTION

Flow control involves the use of passive or active devices to effect changes in wall-bounded or free-shear flows [1]. These devices have been applied in order to increase the flow reattachment performance of separated flow region [2]. The simplest geometry to generate separated flow is a flow over a backward facing step. In fact, substantial research works have been focused on the backward facing step both experimentally [3-6] and numerically [7-9].

Kyoji et. al., [3] conducted an experimental study of the effects of the electromagnetic flap actuators on a separated laminar flow over a backward facing step. He used PIV as an instrument to visualize the flow and heat transfer field distributions. He found that the heat transfer was enhanced significantly by the increase of the flap actuators frequency.

Other researchers that performed similar works are Armaly et. al., [4] and Chun et. al., [5,6]. Both groups used small disturbance introduced into the backward facing step flow in order to control the flow and interesting results have been obtained. Some of them are larger disturbance achieves larger flow modification so that the flow reattachment length is minimized. Other important result that worth to be mentioned is the largest flow modification or the minimum flow reattachment length is obtained at a certain disturbance frequency.

Besides experimental works, numerical works also have been used as a tool to investigate the effectiveness of the flow control over a backward facing step. Among them are Chiang et. al., [7], Kondoh et. al., [8] and Kiwan et. al., [9]. Some of the works were compared with the experimental results (for instance, Chiang et. al., [7]) and they found that the numerical results have fair agreement with the experimental results.

In the current study, the author uses passive skewed vane-type vortex generators to generate longitudinal vortices to suppress flow separation on the backward step surface. Passive Vg does not require any external energy and their system is very simple compared to the active flow control devices. Therefore that can be advantageous as this can significantly reduce the cost of the device.

THE NUMERICAL ANALYSIS

The computational domain

A computational fluid dynamic (CFD) code Fluent™ is used to simulate flow field. Fig. 1 shows the physical domain considered in the current study with boundary conditions and Fig. 2 shows the meshing. In overall, the

computational domain mimics the experimental physical domain. The Reynolds number based on the freestream velocity and the distance from the inlet is varied between 8 x 10^3 to 80 x 10^3. Although the Reynolds number indicates a laminar type of flow, but due to the highly reverse flow that is expected to occur just after the step, the flow is treated as turbulence flow. For the case of Reynolds number of 8 x 10^3, the boundary layer thickness at the *Vg* location is about 1.5 cm and the *Vg* height is about 1/3 from the boundary layer height. The shape of the *Vg* is set to be rectangular in order to ease its fabrication process.

Due to the high skewness angle and to save the meshing time, only unstructured mesh could be used and the total number of meshes is about one million. More meshes are concentrated near the wall surfaces as most of the flow interactions occur in this region and therefore increase the accuracy of the simulations. A mesh dependency check is performed and it is found that the number of mesh is sufficient to predict the flow structures.

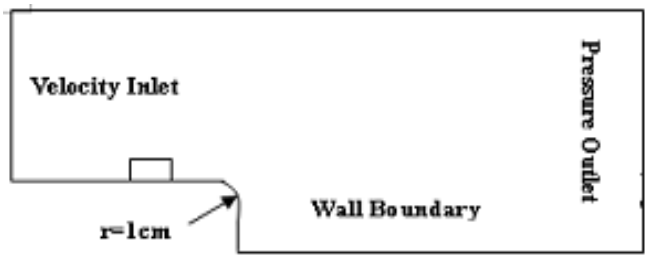

Fig. 1: Computational Domain and Boundary Conditions

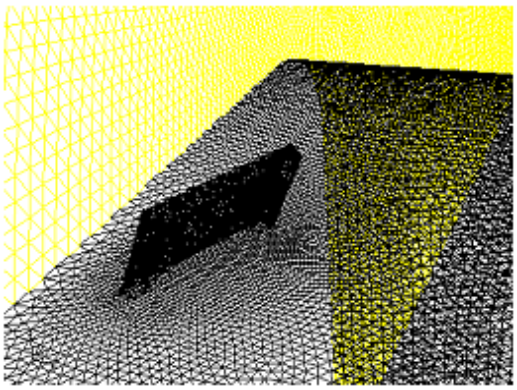

Fig. 2: Unstructured Mesh Surrounding the VG

The Mathematical model

The conservation of mass and momentum equations are written as equation 1 and 2 respectively.

$$\frac{\partial \rho}{\partial t} + \frac{\partial}{\partial x_i}(\rho u_i) = 0 \quad (1)$$

$$\frac{\partial}{\partial t}(\rho u_i) + \frac{\partial}{\partial x_i}(\rho u_i u_j) = -\frac{\partial P}{\partial x_i} + \frac{\partial \tau_{ij}}{\partial x_j} \quad (2)$$

Where $u_{i,j}$ is the flow velocity vector. The first and second terms on the left hand side of equation 2 are the time derivative term and convective term. The terms on the right are the diffuser terms. The computation is performed with an implicit coupled mode; the SIMPLE algorithm is used for pressure-velocity coupling and

second order spatial discretisation is used for all the equations. The choice of second order scheme for discretisation is to obtain higher accuracy.

To reduce the computation time, a simulation of fully developed flow through a two dimensional duct is performed and the velocity profile of the outlet duct is set as the upstream boundary condition for the three dimensional flow.

THE EXPERIMENTAL SETUP

All tests are conducted in an open circuit subsonic wind tunnel as shown in Fig. 3. The flow enters the wind tunnel through a settling chamber containing a honeycomb and three screens which are used for flow conditioning purpose. The tunnel has a test section of size 300 mm x 300 mm x 600 mm, provided with transparent side walls for visualization and measurement purposes. The maximum velocity at the test section is 38 m/s.

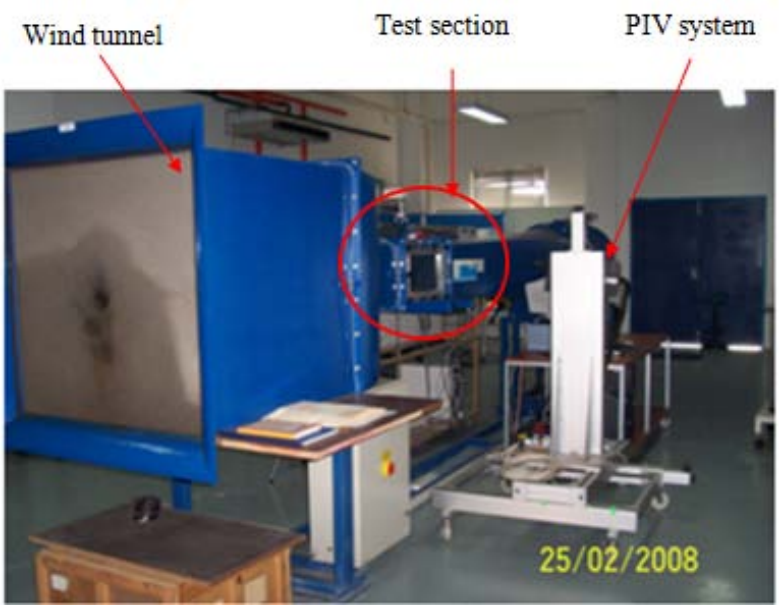

Fig. 3: The experimental setup with open circuit low speed wind tunnel.

A step of 50 mm height is attached inside the test section, which results in expansion ratio (ER) of 1.2. Six pairs of counter-rotating VGs are located at 35 mm upstream the curve of backward facing step. Smoke injector and seeding generator are arranged near the inlet of the wind tunnel to facilitate smoke flow and seeding in the test section. Vegetable based cooking oil is used as the seeding agent.

The parameters of VG are shown in Table 1. In the present study, the BFS with and without VG are investigated with for four different Reynolds numbers corresponding to the mainstream velocities 0.5 m/s, 1.0 m/s, 1.5 m/s and 5 m/s respectively. The parameters of VG relative to boundary layer thickness, h/δ for the upstream condition at X= 150 mm and at room temperature of 27 $^{\circ}C$ are shown in Table 2. The arrangement of VGs in an array is shown in Fig. 4.

Table 1: VG's Parameters

Parameters	h (mm)	L (mm)	l/h	D/h	d/h	Ls/h	$\alpha(^{O})$	$\beta(^{O})$
Value	5	10	2	10	2	5	20	60

Table 2: Physical Properties for the Wind Tunnel Work

Velocity (m/s)	Reynolds number (Re_x)	Boundary layer thickness (δ) cm	h/ δ
0.5	8100	1.47	0.34
1.0	16198	1.04	0.48
1.5	24297	0.85	0.59
5.0	80991	0.47	1.07

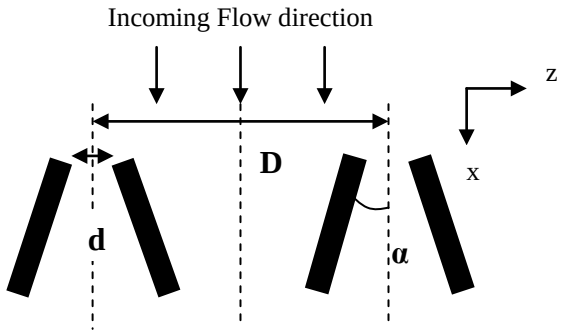

Fig. 4: Top view of the Vg arrangement and parameters

A 2D DANTEC^{TM} PIV system is used in the current investigation as presented in Fig. 5. A laser that produces 50 mJ per pulse with $\pm 4\%$ of energy stability is used. The duration for each pulse is 5 ns. In order to measure a plane in streamwise direction, the laser is set up beside the test section. A mirror is mounted at the top of the test section to divert the laser beam as shown.

A high-speed PIV camera is set on the other side of the wind tunnel test section, to record the images. The camera provides 1600×1186 pixels resolution with 8 bits of dynamic range. The whole PIV operation is carried out by FlowManager V4.60 Software and data acquisition hardware. Above operating parameters for this system are kept constant throughout the experiment.

RESULTS AND DISCUSSION

A comparison was made between the experimental and simulation results. The flow is set to be steady and therefore the transient state of the flow is ignored. Meanwhile for experimental work, the data is obtained instantaneous downstream the step at a mainstream speed of 0.5 m/s.

Figs. 6 (a) and 6 (b) show the longitudinal distribution of velocity vector for flow without vortex generators obtained from experimental and simulation works respectively. Backward-facing step is observed as seen in white color on the right hand-sides of Fig. 6a. In general, both results show identical flow pattern such as occurrence of flow separation, appearance of reverse flow immediately after the backward step, and the flow field far above the step not highly affected.

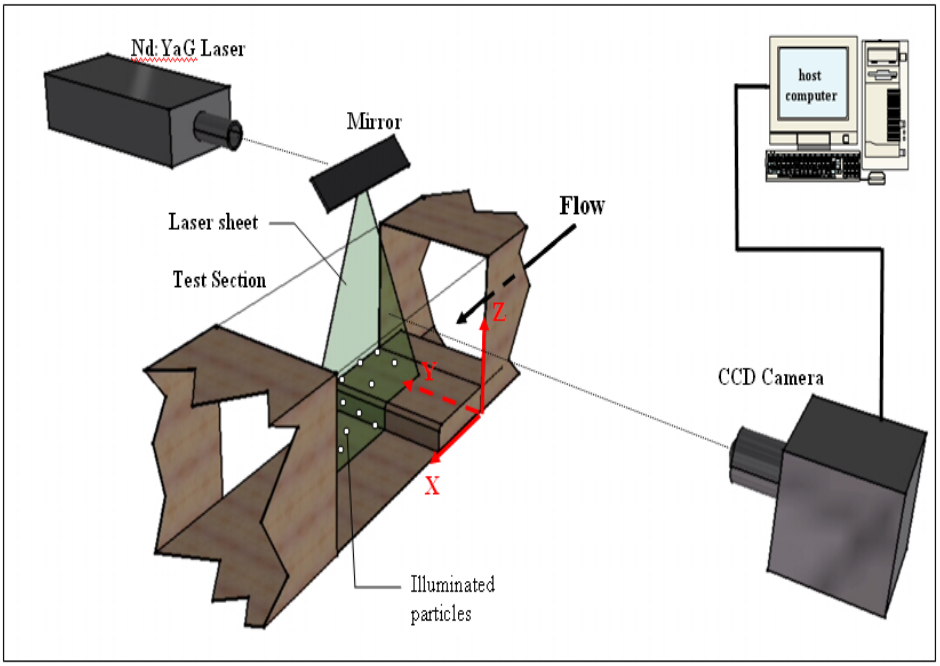

Fig. 5: PIV Wind Tunnel Experimental Setup

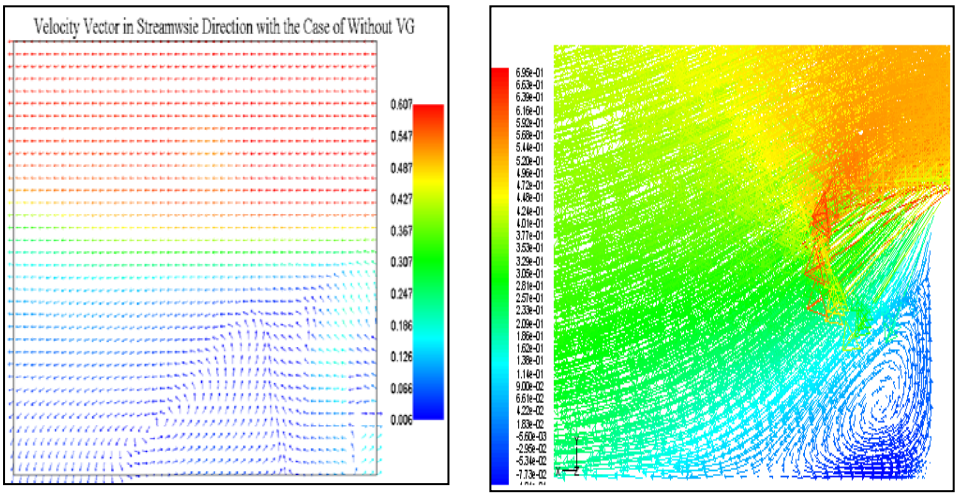

(a) Experimental *(b) Simulation*

Fig. 6: Longitudinal velocity vector distribution for flow without vortex generator

The main feature of the flow is a weak vortex appeared immediately after the step and can be seen in Figs. 6 (a) and (b). This vortex flow entrained some fluid that came near to it and form a dead zone where the trapped fluid cannot flow out from the vortex flow area. Reattachment length of the separated flow is 137 mm for the experimental study and 175 mm for simulations, the difference being 20%, is reasonable.

Figs. 7 (a) and (b) show the longitudinal distribution of velocity vector for flow with vortex generators, obtained from experimental and simulation works respectively. Similar to the case of flow without vortex generators, both cases show identical features macroscopically. Reattachment length of the separated flow is 101.6 mm the experiment and 165 mm for simulations with the acceptable difference of about 35%. Comparison of flows with and without vortex generators reveals that the skewed vortex generators could suppress the flow separation up to 25%.

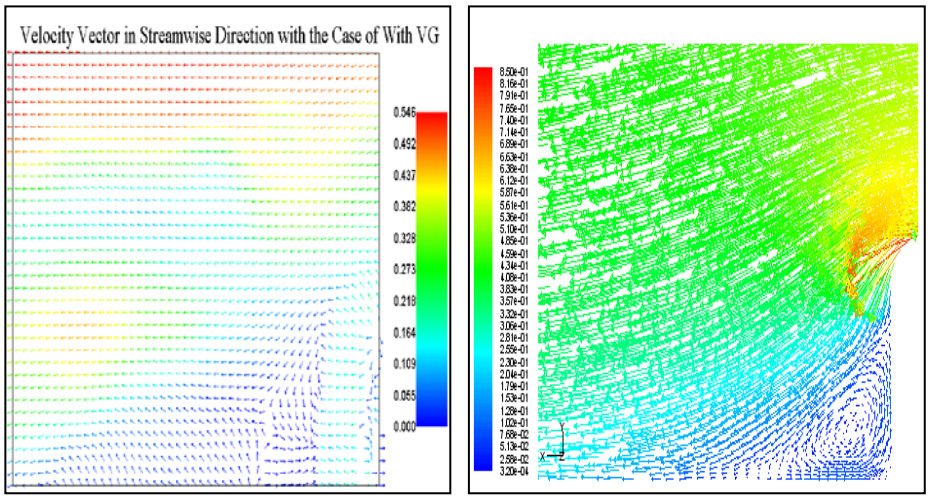

(a) Experimental *(b) Simulation*

Fig. 7: Longitudinal velocity vector distribution for flow with vortex generator

It is noted that there is a discrepancy between experimental and CFD results. This may be attributed to, 1) in CFD, the mesh is fully unstructured, and therefore may contribute to the diffusion error of the simulations and 2) the seeding material used in the experiments may not be appropriate as it could not cover enough particles in the vortex flow area for the flow measurements. Both problems cannot be improved in the current works due to, 1) in CFD, the skewness angle of the Vg prevents the author to generate structured mesh around the Vg and therefore this is unavoidable and 2) as the current works only involved low speed flow, therefore a light material such as vegetable oil is suitable compared to the heavier seeding materials.

Figs. 8 and 9 show the zero velocity line for flows without and with vortex generators respectively. A reattached flow is achieved when the lines (dotted and solid) in the graphs reaching zero and the backward step is located at 80 mm location. For flow without vortex generators (Fig. 8), only flow with velocity of 0.5 m/s has tendency to reattach to the floor of the test section. Although the other cases have a declining feature (notice that the lines in the graph for other cases are also declining) for the first 50 mm downstream of the step, they start to diverge afterwards. Meanwhile the flows with vortex generators have tendency to reattach to the floor of the test section (Fig. 9) at all velocities. This shows that vortex generators managed to suppress the separation flow regardless of velocity (range from 0.5 m/s to 5 m/s).

Figs. 10 and 11 show the comparison of normalized streamwise velocity profiles for different incidence angles at two span-wise locations, Z = 5 mm and Z = 7.5 mm respectively. From Fig. 10, it can be seen that VG with all configurations produce fuller velocity profiles compared to the uncontrolled case. VG with 20 degree of incidence produces the fullest velocity profile compared to the other two cases. The fuller velocity profile at this location is due to high momentum-transfer of fluid particles from upper level of flow towards the lower level which is near to the bottom surface. This motion is induced by the induced vortices. As the induced vortices move downstream, the strength of the induced vortex diffuses, resulting in thinner profiles as observed.

From Fig. 10, it can be seen that all VG cases produce thinner velocity profile compared to the uncontrolled case. This is due to the fact that this span-wise location is the up-wash region where low momentum fluid particles are transferred from lower level of flow towards upper level. It can also be noticed that there is no significant difference between VG cases.

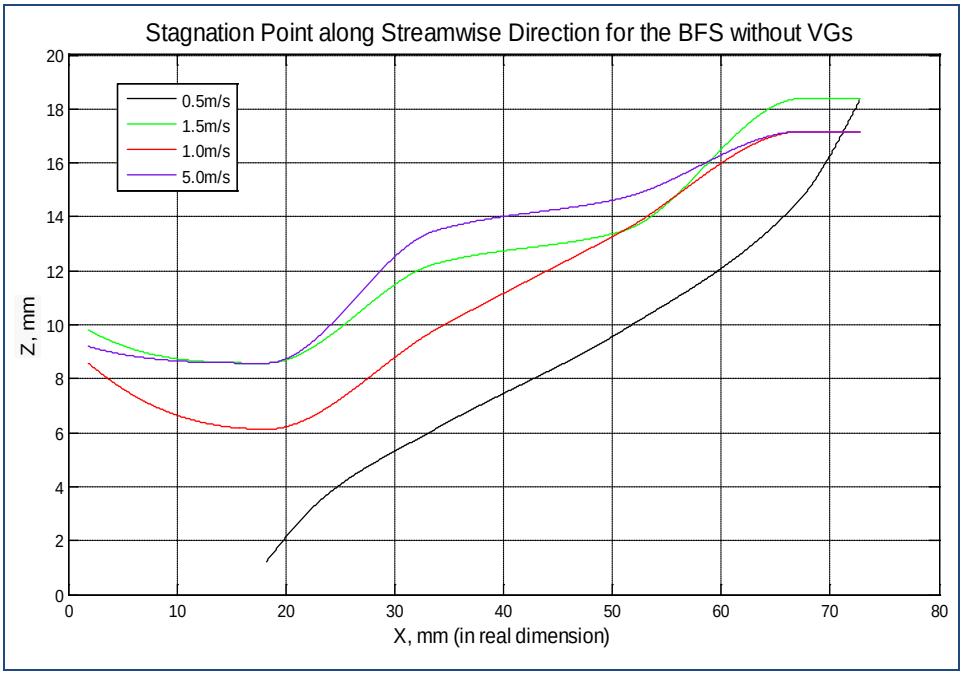

Fig. 8: Zero Velocity Line for the Flow Downstream of the Step without VG

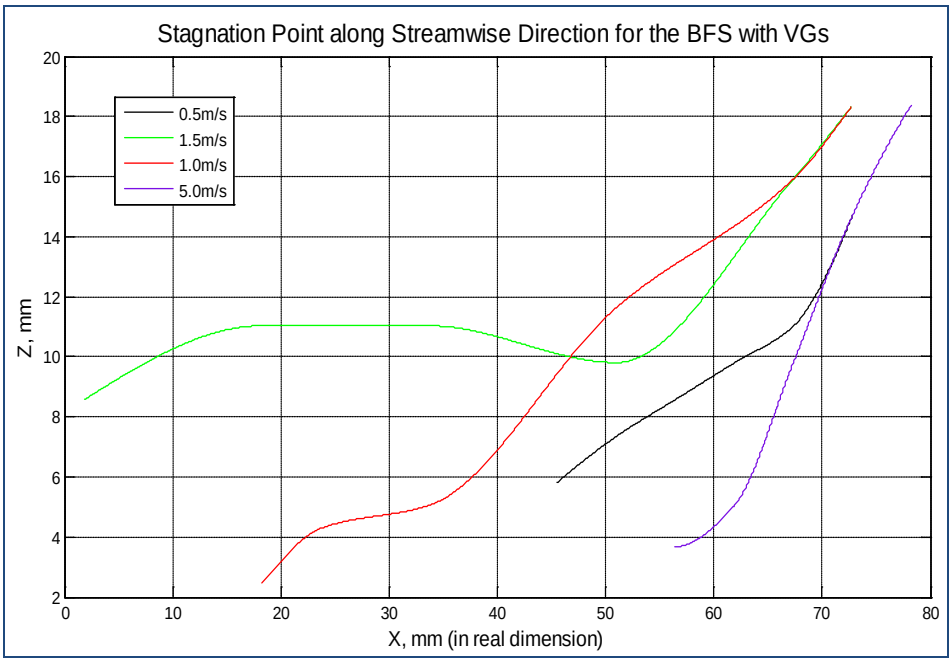

Fig. 9: Zero Velocity Line for the Flow Downstream of the Step with VG

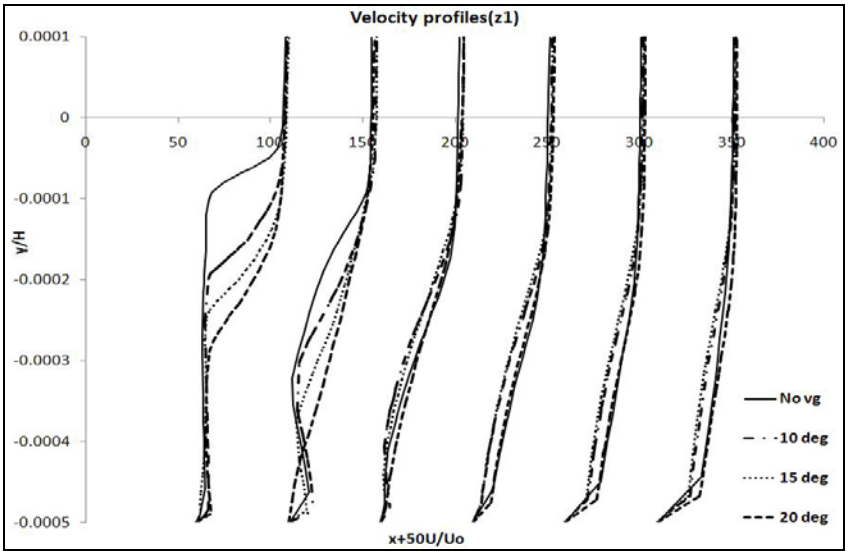

Fig. 10: Normalized streamwise velocity profiles at z = -5 mm at different x locations

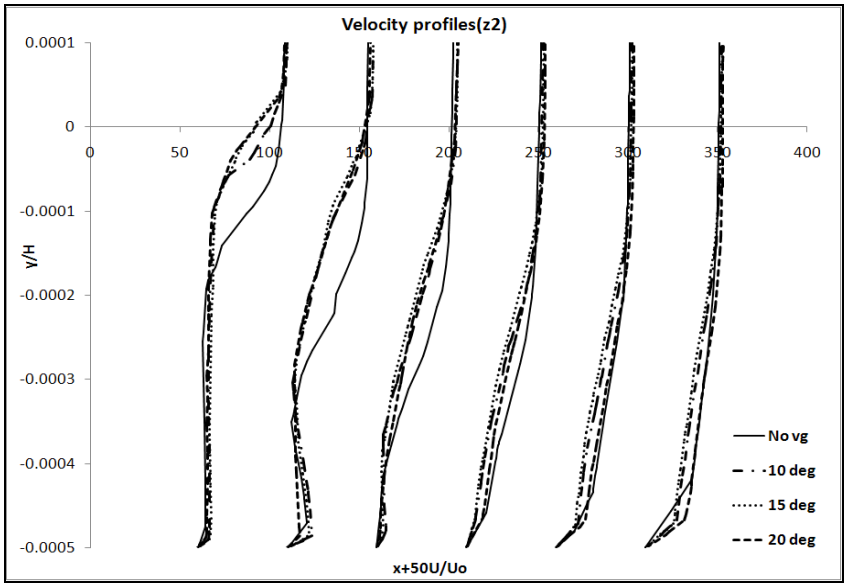

Fig. 11: Normalised streamwise velocity profiles at z = 7.5 mm at different x locations

CONCLUSION

An array of passive vortex generators with the skewness concept is investigated for controlling the flow separation downstream of the backward-facing step. The 3D simulation is performed by RANS code FLUENT 6^{TM} to predict the flow fields using a hybrid mesh with k-ε turbulence model and standard wall function. The numerical analysis is satisfactorily compared by experiments performed by using a particle image velocimetry (PIV) system. The results show that the proposed vortex generators greatly enhance the flow mixing between the separation area and the mainstream flow. However there is a scope for improvement of the current study, to arrive at more realistic results. The experimental results could be improved by choosing appropriate seeding material such as high-powered smoke generator. This work may be extended for the application of the skewed vortex generators on aerodynamics shapes such as wings or flaps.

ACKNOWLEDGEMENT

The author would like to thanks Universiti Sains Malaysia for sponsoring the work under Research University Grant (Account Number: 814042) and providing the facilities for the experimental and numerical works.

REFERENCES

[1] Gad-El-Hak, M. (2000) Flow Control: Passive, Active, and Reactive flow management. Cambridge University Press London.

[2] Lin, J.C. (2002) Review of research on low-profile vortex generators to control boundary-layer separation. Progress in Aerospace Sciences. 38: 389-420,

[3] Kyoji Inaoka, Kazuya Nakamura and Mamoru Senda (2004) Heat transfer control of a backward-facing step flow in a duct by means of miniature electromagnetic actuators. International Journal of Heat and Fluid Flow. 25: 711-720.

[4] Armaly, B.F., Durst, F., Pereira, J.C.F. and Schonung, B. (1983) Experimental and theoretical investigation of backward-facing step flow. Journal of Fluid Mechanics. 127: 473–496

[5] Chun, K.B. and Sung, H.J. (1996) Control of turbulent separated flow over a backward-facing step by local forcing. Experiments in Fluids. 21: 417–426.

[6] Chun, S., Lee, I. and Sung, H.J.(1999) Effect of spanwise-varying local forcing on turbulent separated flow over a backward-facing step. Experiments in Fluids. 26: 437–440

[7] Chiang, T.P. and Sheu, T.W.H. (1999) A numerical revisit of backward-facing step flow problem. Physics of Fluids. 11: 862–874.

[8] Kondoh, T., Nagano, Y. and Tsuji, T. (1993) Computational study of laminar heat transfer downstream of a backward-facing step. International Journal of Heat and Mass Transfer. 36: 577–591.

[9] Kiwan, S. (2008) Using localized wall discharge to control the fluid flow and heat transfer for the flow over a backward facing step. International Journal of Numerical Methods for Heat and Fluid Flow. 18: 745-765

NOMENCLATURE

BFS	Backward Facing Step	
B	Skewness angle	degree
c	Length of the *Vg*	mm
CFD	computational fluid dynamics	
D	distance between a pair of counter-rotating Vgs	mm
D	distance between two pair of Vgs	mm
∂	partial differential equation	
Δ	boundary layer thickness	mm
H	Vg's height	mm
Ls	Position of Vg upstream of the baseline separation	mm
u	velocity vector	m/s
U_∞	freestream velocity	m/s
P	density	kg/m^3
P	pressure	Pascal
Re_x	Reynolds number	
t	time	sec
x	longitudinal distance	mm